

Recent Activities at Laboratory of Experimental Nuclear and Particle Physics

G. N. Kim^{1,*}, M. W. Lee¹, K. S. Kim¹, K. Kim¹, S. C. Yang¹, T. I. Ro², Y. R. Kang², H. S. Kang³, M. H. Cho³, I. S. Ko³, and W. Namkung³

¹*Department of Physics, Kyungpook National University, Daegu 702-701, Korea*

²*Department of Physics, Dong-A University, Busan 604-714, Korea*

³*Pohang Accelerator Laboratory, Pohang University of Science and Technology, Pohang 790-784, Korea*

**email:gnkim@knu.ac.*

We report the activities by using the pulsed neutron facility which consists of an electron linear accelerator, a water-cooled Ta target with a water moderator, and a 12 m time-of-flight path. It can be possible to measure the neutron total cross-sections in the neutron energy range from 0.01 eV to few hundreds eV by using the neutron time-of-flight method. A ⁶LiZnS(Ag) glass scintillator was used as a neutron detector. The neutron flight path from the water-cooled Ta target to the neutron detector was 12.1 m. We also report the nuclear data production experiments by using the activation methods with neutron and bremsstrahlung beams from the electron linac of Pohang Accelerator Laboratory.

1. Introduction

Electron linear accelerators (linac) are being used throughout the world in a variety of important applications. The pulsed neutron facility based on an electron linac is effective for measuring energy dependent cross-sections with high resolution by the time-of-flight (TOF) technique covering the energy range from thermal neutrons to a few tens of MeV. The measurement of neutron cross-sections gives basic information about the internal structure of atomic nuclei and their constituents. Precise measurements of neutron cross-sections are of great importance for the safety design of nuclear reactors and for the evaluation of the neutron flux density and the energy spectrum around a reactor.

The Pohang Neutron Facility (PNF) based on a 100-MeV electron linac was proposed in 1997 and constructed at the Pohang Accelerator Laboratory (PAL) on December 1998 [1]. Its main goal is to construct the infrastructure for the nuclear data production in Korea.

Recently, the PNF has been used for measuring the cross-sections of neutron-nucleus reactions and photo-nucleus reactions.

2. Pohang Neutron Facility

The Pohang Neutron Facility (PNF) consists of an electron linac, a water-cooled Ta target, and a ~12-m-long TOF path. The characteristics of the facility are described elsewhere [2]. The beam energy of the electron linac is varied from 75 MeV to 50 MeV, and the beam currents at the end of linac are in between 100 mA and 30 mA. The length of electron beam pulse is 1-2 μ s, and the pulse repetition rate is 10 Hz.

A Ta target was designed and constructed for the neutron production by way of bremsstrahlung under high power electron beams [3]. The Ta target was composed of ten Ta sheets, 49 mm in diameter and 74 mm in total length. There was 1.5 mm water gap between Ta sheets in order to cool the target effectively. The target housing was made of 0.5 mm thick

titanium. The estimated neutron yield per kW of beam power at the neutron target was about 10^{12} n/sec.

The neutron guide tubes were constructed of stainless steel with two different diameters, 15 cm and 20 cm, and were placed perpendicularly to the electron beam. The neutron collimation system was mainly composed of H_3BO_3 , Pb, and Fe collimators, which were symmetrically tapered from a 10-cm diameter at the beginning to a 5-cm in the middle position where the sample was located, to an 8-cm diameter at the end of guide tube where the neutron detector was placed. There was 1.8-m-thick concrete between the target and the detector room.

During the experiment, the electron linac was operated with a repetition rate of 10 Hz, a pulse width of 1.0 μ s, and the electron energy of 60 MeV. The peak current in the beam current monitor located at the end of the second accelerator section is above 50 mA, which almost is the same as that in the target.

3. Nuclear Data Measurement

3.1 With Neutron TOF Method

The experimental arrangement for the neutron total cross-section measurements by using the neutron TOF method, which is similar to the previous one [4], is shown in Fig. 1. The target is located at a position where the electron beam hits its center. To reduce the gamma flash generated by the electron burst in the target, the target is placed in 5.5 cm away from the center of the neutron guide to the backward direction. This target was set in the cylindrical water moderator contained in an aluminum cylinder with a thickness of 0.5 cm, a diameter of 30 cm and a height of 30 cm. The water level in the moderator was 3 cm above the target surface which was decided by the measurement of thermal neutron flux and also compared with the Monte Carlo simulation [3].

A high purity (99.99%) natural niobium metallic plate with a diameter of 80.11 ± 0.01 mm and the thickness of 15.04 ± 0.03 mm, was placed at the midpoint of the flight path. A set of notch filters of Co, In, and Cd plates with 0.5, 0.2, and 0.5 mm in thickness respectively, was used for the background measurement and the energy calibration.

The neutron detector was located at a distance of 12.06 ± 0.02 m from the photo-neutron target. A ${}^6\text{Li}$ -ZnS(Ag) scintillator BC702 from Bicron (Newbury, Ohio) with a diameter of 125 mm and a thickness of 16 mm mounted on an EMI-93090 photomultiplier was used as a detector for the neutron TOF spectrum measurement. This scintillator consists of a matrix of a lithium compound enriched to 95% ${}^6\text{Li}$ dispersed in a fine ZnS(Ag) phosphor powder.

The configuration of the data acquisition system used in this measurement is also shown in Fig. 1. The details of data acquisition system and data taking are described elsewhere [2].

In the transmission measurements, we have taken data with sample in and out (open beam) periodically. Total data taking times for sample in and out are 35.83 hours. The neutron total cross section is determined by measuring the transmission of neutrons through the sample. The transmission rate of neutrons at i -th group energy E_i is defined as the fraction of incident neutrons passing through the sample compared to that in the open beam. Thus, the neutron total cross-section is related to the neutron transmission rate $T(E_i)$ as follows:

$$\sigma(E_i) = -\frac{1}{\sum_j N_j} \ln T(E_i), \quad (1)$$

$$T(E_i) = \frac{[I(E_i) - IB(E_i)]/M_I}{[O(E_i) - OB(E_i)]/M_O} \quad (2)$$

where N_j is the atomic density per cm^2 of j -th isotope in the sample. $I(E_i)$ and $O(E_i)$ are the foreground counts, $IB(E_i)$ and $OB(E_i)$ are the background counts, and M_I and M_O are monitor counts for sample in and out, respectively. In this measurement, we assumed the monitor counts to be equal during the experiment.

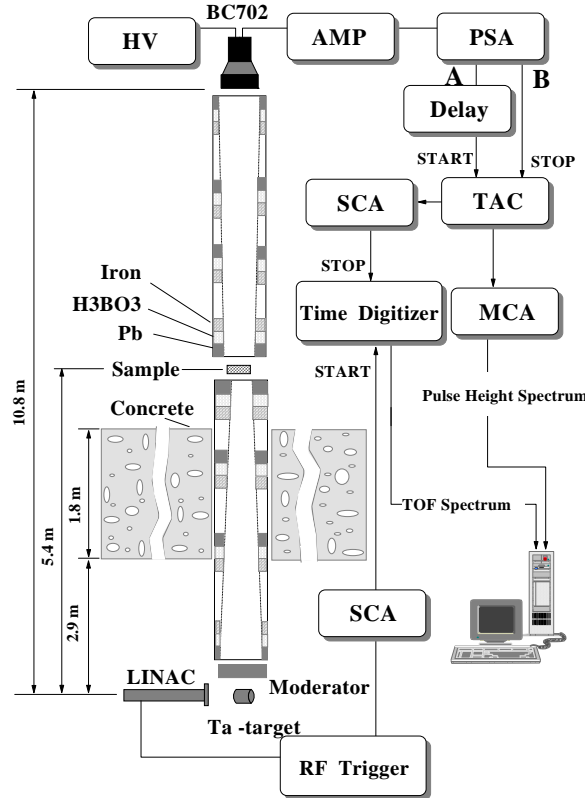


Fig. 1 Experimental arrangement and a block diagram for data acquisition.

The total cross-sections for several samples (Mo, Ta, Hf, Dy, In, and Cu) as a function of neutron energy were obtained and published in [4, 5]. The statistical error can be determined from Eq. (1) assuming the monitor counters are equal during the measurements. The systematic uncertainties came from the following sources: the sample thickness, and the dead time, the normalization, and so on.

3.2 With Neutron Activation Method

The thermal neutron cross-sections and the resonance integrals of several (n,γ) reactions have been measured with the neutron activation method by using a $^{197}\text{Au}(n,\gamma)^{198}\text{Au}$ monitor reaction as single comparator. The high-purity natural samples and gold monitor samples with and without a cadmium shield case of 0.5 mm thickness were irradiated in a neutron field of the PNF. The details of the experimental procedure are described elsewhere [6-8].

The thermal neutron cross-section for the $^A\text{S}(n,\gamma)^{A+1}\text{S}$ (A is mass number and S is sample) reaction, $\sigma_{0,S}$, has been determined relative to that for the $^{197}\text{Au}(n,\gamma)^{198}\text{Au}$ standard reaction as follows [9]:

$$\sigma_S = \sigma_{Au} \cdot \frac{R_S - F_S^{Cd} R_S^{Cd}}{R_{Au} - F_{Au}^{Cd} R_{Au}^{Cd}} \cdot \frac{G_{Au}}{G_S} \cdot \frac{g_{Au}}{g_S}, \quad (3)$$

where σ_{Au} is the thermal neutron cross-section of the $^{197}\text{Au}(n,\gamma)^{198}\text{Au}$ reaction, R_x and R_x^{Cd} are reaction rates per atom for bare and Cd-covered x (S or Au) isotope irradiation, respectively. The cadmium correction factor, F_x^{Cd} accounts for the difference in count rates for Cd covered and bare samples, and G_x is the thermal neutron shielding factor for x samples. The Westcott factor g_x , is the correction for the departure from $1/v$ cross-section behavior for neutron capture reactions of x samples. The reaction rates R_x and R_x^{Cd} are determined by measuring the activities of emitted γ -ray from the (n,γ) reaction. The emitted γ -ray was chosen with high intensity, well separated, and relatively low background.

The resonance integral for the (n,γ) reaction in an ideal $1/E$ epithermal neutron spectrum is defined by the following relation:

$$I_S = \int_{E_{Cd}}^{\infty} \frac{\sigma(E)}{E} dE, \quad (4)$$

where $\sigma(E)$ is the cross-section as a function of neutron energy E , and E_{Cd} is the cadmium cut-off energy, which is usually defined as 0.55 eV. The resonance integral defined in Eq. (4) is not valid in a non-ideal, real epithermal neutron spectrum [9]. The resonance integral of a $1/E^{1+\alpha}$ real epithermal neutron spectrum for $^A\text{S}(n,\gamma)^{A+1}\text{S}$ reaction has been determined relative to that for the $^{197}\text{Au}(n,\gamma)^{198}\text{Au}$ reaction as a standard by the following relation:

$$I_S(\alpha) = I_{Au}(\alpha) \cdot \frac{g_S \sigma_S}{g_{Au} \sigma_{Au}} \cdot \frac{CR_{Au} - F_{Au}^{Cd}}{CR_S - F_S^{Cd}} \cdot \frac{G_{Au}^{epi} G_S}{G_{Au}^{epi} G_S}, \quad (5)$$

where α is an epithermal neutron spectrum shaping factor, which is energy dependent, and G_x^{epi} is the epithermal neutron self-shielding factor for x (sample S or Au) sample. Then, the obtained $I_S(\alpha)$ value was converted to I_S by the relation given as [9]:

$$I_S(\alpha) = \left[\frac{I_S - 0.426g\sigma_S}{(\bar{E}_r)^\alpha} + \frac{0.426g\sigma_S}{(2\alpha+1)(E_{Cd})^\alpha} \right], \quad (6)$$

where \bar{E}_r effective resonance energy (eV), as defined by Ryves and Paul [10], the term $(I_S - 0.426g\sigma_S)$ represents the reduced resonance integral, i.e. with the $1/v$ tail subtracted. In order to improve the accuracy of the experimental results, the following correction factors such as the neutron self-shielding, the γ -ray attenuation, the cadmium correction, and the g -factor were considered.

We measured the thermal neutron cross-sections and the resonance integrals for the $^{179}\text{Hf}(n,\gamma)^{180\text{m}}\text{Hf}$ and $^{180}\text{Hf}(n,\gamma)^{181}\text{Hf}$ reactions [6], the $^{186}\text{W}(n,\gamma)^{187}\text{W}$ reaction [7], and the $^{98}\text{Mo}(n,\gamma)^{99}\text{Mo}$ reaction [8]. The new measurements for the $^{165}\text{Ho}(n,\gamma)^{166\text{g}}\text{Ho}$ reaction are presented in here. The thermal neutron cross-section and the resonance integral for the $^{165}\text{Ho}(n,\gamma)^{166\text{g}}\text{Ho}$ reaction are $\sigma_{Ho} = 59.7 \pm 2.5$ barn and $I_{Ho} = 671 \pm 45$ barn, respectively.

3.3 With Gamma Activation Method

We measured the isomeric yield ratios for the isomeric pairs produced from various photo-nuclear reactions by using the gamma activation method. We used bremsstrahlung photons with the end point energy 50-, 60-, 65-, and 70-MeV produced from an electron linac of the PNF. The experimental procedure for measuring the isomeric yield ratios for various samples at this facility with varying the end point energy of the bremsstrahlung were found in elsewhere [11-14]. The bremsstrahlung is produced when a pulsed electron beam hit a 0.1-mm thin W-target with a size of 100 mm × 100 mm. The W-target is located at 18 cm from the beam exit window. The high-purity metallic foils of natural composition were exposed to uncollimated bremsstrahlung of 50-, 60-, 65-, and 70-MeV. The activation foils were placed in air at 12 cm from the W target and they were positioned at zero degree with the direction of the electron beam. The time of sample irradiation is considered according to the half-lives of the reaction products. The spectroscopic measurements of the studied nuclei from the activated foils were taken with a p-type coaxial CANBERRA high-purity germanium (HPGe) detector which is operated with GENIE2000 data acquisition software. The full peak efficiency was measured with standard radioactive source. The details of the detection efficiency measurement as a function of photon energy are given in [11].

In activation process, considering the production of nuclide of isomeric state and ground state at the same time of irradiation and internal transfer, we can derive the isomeric yield ratio IR from the measured gamma activities as $IR = Y_m/Y_g$, where $Y_{m(g)}$ is the yield of the isomeric- and the ground-state. In case of the bremsstrahlung irradiation, due to the continuity of the energy spectrum, the population of the isomeric and the ground state yields can be expressed as follows:

$$Y_i = N_0 \int_{E_{th}}^{E_{\gamma, \max}} \sigma_i(E) \phi(E) dE, \quad (7)$$

where i represents the isomeric state (m) or ground state (g) of a isomeric pair product of interest, N_0 is the number of target nuclei, $\sigma_i(E)$ is the energy dependent reaction cross-section and $\phi(E)$ is the shape of the bremsstrahlung spectrum. $E_{\gamma, \max}$ and E_{th} are the maximum end point energy of bremsstrahlung and the reaction threshold, respectively.

We measured the isomeric yield ratios for the $^{45}\text{Sc}(\gamma, n)^{44\text{m,g}}\text{Sc}$ reaction, the $^{nat}\text{Ti}(\gamma, x)^{44\text{m,g}}\text{Sc}$ reaction, the $^{103}\text{Rh}(\gamma, 4n)^{99\text{m,g}}\text{Rh}$ reaction, the $^{nat}\text{Fe}(\gamma, x)^{52\text{m,g}}\text{Mn}$ reaction, the $^{197}\text{Au}(\gamma, n)^{196\text{m,g}}\text{Au}$ reaction, the $^{nat}\text{In}(\gamma, xn)^{110\text{m,g}}\text{In}$, $^{111\text{m,g}}\text{In}$, $^{112\text{m,g}}\text{In}$ reactions, and the $^{nat}\text{Sn}(g, xnp)^{117\text{m,g}}\text{In}$ reaction using 50-, 60-, 70-MeV bremsstrahlung [11-14].

As an example, the isomeric yield ratios of $^{44\text{m,g}}\text{Sc}$ from ^{45}Sc are measured by the gamma activation method with the maximum bremsstrahlung energy ($E_{\gamma, \max}$) of 50-, 60-, and 70-MeV. The $^{44\text{m,g}}\text{Sc}$ isomeric pair were identified based on their characteristic γ -ray energies and half-lives. The nuclear reactions and decay data of the $^{44\text{m,g}}\text{Sc}$ are taken from [15]. According to the decay scheme given in [15], the isomeric state $^{44\text{m}}\text{Sc}$ (high spin state, 6^+) with a half-life of 58.6 h decays directly to the 3285.0 keV state of ^{44}Ca (6^+) by an electron capture reaction with a branching ratio of 1.20%. Meanwhile, 98.8% of the isomeric state decays to the unstable ground state $^{44\text{g}}\text{Sc}$ (low spin state, 2^+) by emitting a 271.13 keV γ -ray. The unstable ground state $^{44\text{g}}\text{Sc}$ (2^+) with a half-life of 3.927 h again decays to the 1157.03 keV energy level of ^{44}Ca (2^+) by both an electron capture and a β^+ -process with a branching ratio of 98.95%. In this work, the activity of the isomeric state, $^{44\text{m}}\text{Sc}$ was determined by using the 271.13 keV γ -ray, and that of the unstable ground state radionuclide $^{44\text{g}}\text{Sc}$ was determined by

using the γ -ray of 1157.03 keV. The interference and coincidence summing are taken in to account in analyzing data. The isomeric yield ratios for the $^{45}\text{Sc}(\gamma, n)^{44\text{m.g}}\text{Sc}$ reaction measured at 50-, 60-, and 70-MeV bremsstrahlung energies are 0.20 ± 0.02 , 0.21 ± 0.02 , and 0.21 ± 0.02 , respectively. The uncertainties were calculated by using the error propagation principle. The main sources of the errors for the present results are due to statistical error (1-3%), uncertainties in photopeak efficiency calibration (2-4%), nuclear data such as half-life, gamma intensity, IT (1-2%), photopeak area determination (1-3%), coincidence summing (2-5%), bremsstrahlung flux fluctuation (1-2%), and others (2-5%). We plotted the present results measured at 50-, 60-, and 70-MeV bremsstrahlung energies together with the reference data [11, 16-21] as shown in Fig. 2. It is shown that the isomeric yield ratios for the $^{45}\text{Sc}(\gamma, n)^{44\text{m.g}}\text{Sc}$ reaction increase rapidly with the increasing bremsstrahlung energies from the reaction threshold up to giant dipole resonance region about 20-30 MeV, and then those values are almost constant in the energy region from about 30 MeV up to 2.5 GeV. That is understandable because the yield for the simple (γ, n) photonuclear reaction was contributed mainly from the giant dipole resonance [20, 22]. Recently, Thiep et al. [23] reported the isomeric yield ratios of a $^{85\text{m.g}}\text{Sr}$ isomeric pair from the $^{\text{nat}}\text{Sr}(\gamma, xn)^{85\text{m.g}}\text{Sr}$ reaction with the bremsstrahlung end-point energies from the giant dipole resonance region to 65 MeV, and it showed the similar trend what we observed. The increasing ratios can be explained as the increasing transfer momentum to the compound nuclei. The flattening out may be due to the increasing importance of reactions from the direct characteristics with particles emitted, which carry off a larger fraction of energy and angular momentum.

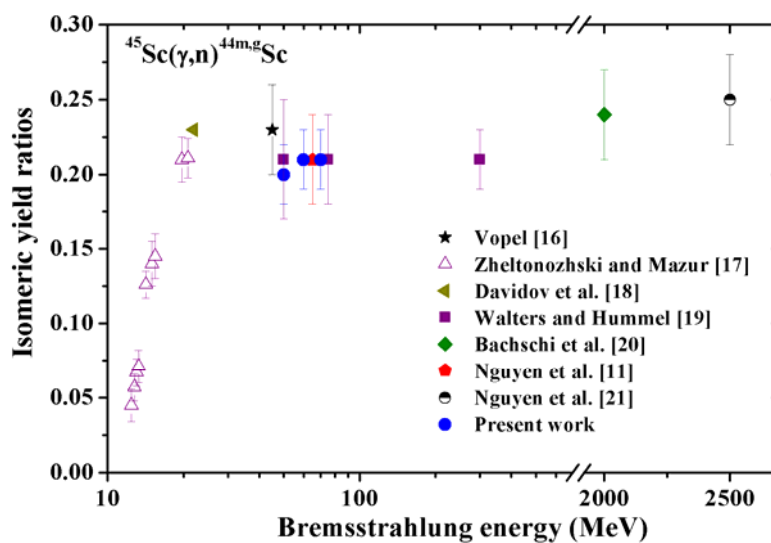


Fig. 2 Isomeric yield ratios of $^{44\text{m.g}}\text{Sc}$.

4. Discussion and Summary

The Pohang Neutron Facility based on an electron linac was constructed for nuclear data production in Korea. It consists of a 100-MeV electron linac, a water cooled Ta target, and an 12-m long TOF path. We measured neutron total cross-sections with neutron TOF method since 2001 cooperated with users came from both Korea and foreign countries. We measured thermal neutron capture cross-sections and resonance integrals with neutron activation method. We also measured isomeric yield ratios for various radioisotopes by using the bremsstrahlung produced by electron linac.

Based on the present activities and experiences obtained during the experiment, we need to upgrade the electron accelerator and construct 4π γ -detection system in order to measure neutron capture cross-sections.

Acknowledgement

The authors would like to express their sincere thanks to the staffs of Pohang Accelerator Laboratory for excellent operation of the electron linac and their strong support. This work was supported by the National Research Foundation of Korea (NRF) through a Grant provided by the Korean Ministry of Education, Science and Technology (MEST) in 2010 (Project No. 2010-0018498 and 2010-0021375), by the Institutional Activity Program of Korea Atomic Research Institute.

References

- [1] G. N. Kim *et al.*, "Proposed neutron facility using 100-MeV electron linac at Pohang Accelerator Laboratory," Proc. Nuclear Data for Science and Technology, Trieste, May 19-24, 1997, p. 556, Italy (1997).
- [2] G.N. Kim *et al.*, J. Korean Phys. Soc. 43, 479 (2003).
- [3] G.N. Kim *et al.*, Nucl. Instr. Meth. A **485**, 458 (2002); K. Devan *et al.*, J. Korean Phys. Soc. 49, 89 (2006).
- [4] T.F. Wang *et al.*, Nucl. Instr. Meth. B 268, 106 (2010); T.F. Wang *et al.*, Nucl. Instr. Meth. B 266, 561 (2008).
- [5] V. Skoy *et al.*, J. Korean Phys. Soc. **41**, 314 (2002); G.N. Kim *et al.*, Ann. Nucl. Energ. 30 (2003) 1123; A.K.M.M.H. Meaze *et al.*, J. Korean Phys. Soc. 46 (2005) 401; A.K.M.M.H. Meaze *et al.*, J. Korean Phys. Soc. 48 (2006) 827.
- [6] V.D. Nguyen *et al.*, Nucl. Instr. Meth. B 266 (2008) 21.
- [7] V.D. Nguyen *et al.*, Nucl. Instr. Meth. B 266 (2008) 863.
- [8] V.D. Nguyen *et al.*, Nucl. Instr. Meth. B 267 (2009) 462.
- [9] F. De Corte *et al.*, J. Radioanal. Chem. 62 (1981) 209.
- [10] T. B. Ryves, E. B. Paul, J. Nucl. Energy 22 (1968) 759.
- [11] V. D. Nguyen *et al.*, J. Korean Phys. Soc. 50 (2007) 417.
- [12] Md. S. Rahman *et al.*, Nucl. Instr. Meth. B 267 (2009) 3511.
- [13] V. D. Nguyen *et al.*, J. Radioanal. Chem. 283 (2010) 683.
- [14] Md. S. Rahman *et al.*, J. Radioanal. Chem 283 (2010) 519.
- [15] R.B. Firestone *et al.*, "Table of Isotopes, Update on CD ROM, 8th edition" Wiley-Interscience, New York, (1999).
- [16] R. Volpel, Nucl. Phys. A 182 (1972) 411.
- [17] V. A. Zheltonozhski and V. M. Mazur, Yad. Fiz. 63 (2000) 389.
- [18] M. G. Davidov, V. G. Magera, A. V. Trukhov, and E. M. Shomurodov Atom. Energy 58 (1985) 47.
- [19] W. B. Walters and J. P. Hummel, Phys. Rev. 150 (1966) 867.
- [20] N. M. Bachschi *et al.*, Nucl. Phys. A 264 (1976) 493.
- [21] V. D. Nguyen *et al.*, Nucl. Instr. and Meth. B 266 (2008) 5080.
- [22] W. Gunther *et al.*, Nucl. Phys. A 297 (1978) 254.
- [23] T. D. Thiep *et al.*, J. Radioanal. Nucl. Chem (2010) DOI 10.1007/s10967-010-0630-5.